Hg–Hg bond will disappear, producing HgX^+ and displacing a Hg atom. The HgX^+ ion, a Hg(II) species, is expected to use sp-hybrid orbitals and will eventually react with another mole of X^- to produce a linear two-coordinate HgX_2 molecule.

It is tempting to try to correlate the energy of the ${}^1\Sigma_u^+ \rightarrow \Sigma_u^+(a^1\Sigma_u^+)$ transition with a dissociation energy of $Hg_2(H_2O)_2^{2+}$ in solution, but such a correlation is difficult at best, and only a crude upper limit estimate could be made and then only if the $\Sigma_u^+(a^1\Sigma_u^+)$ state is an unbound state. If it is a bound state, then no correlation can be made at all. The broadness of band I may signal an unbound state, but the broadness may be nothing more than unresolved vibrations in a room-temperature solution spectrum. Further, the uncertainty of the energy difference between the $\Sigma_u^+(a^1\Sigma_u^+)$ state and the dissociation limit of the ground state, together with differences in solvation energies of the undissociated and dissociated ions, preclude any sound quantitative estimate of the Hg–Hg bond energy.

Acknowledgment is made to the donors of the Petroleum Research Fund, administered by the American Chemical Society, for the support of this research.

Registry No. $[Hg_2(H_2O)_2](ClO_4)_2$, 83546-48-9; $Hg_2(H_2O)_2^{2+}$, 56650-84-1.

Contribution from the Department of Chemistry,
Northeastern University, Boston, Massachusetts 02115

Thiocyanate-Bridged Transition-Metal Polymers. 4. A Study of the Structural, Electronic, and Magnetic Properties of Some Mono(2,2′-bipyridyl) Transition-Metal Thiocyanates: Zigzag Polymeric Chains Based on $Mn(bpy)(NCS)_2$ and $Co(bpy)(NCS)_2$

BRUCE W. DOCKUM, GLENN A. EISMAN, E. H. WITTEN, and WILLIAM MICHAEL REIFF*

Received February 12, 1982

$Mn(bpy)(NCS)_2$ and $Co(bpy)(NCS)_2$ (bpy = 2,2′-bipyridine) have been prepared by the thermolytic decomposition of the corresponding monomeric bis(bipyridyl) complex, $M(bpy)_2(NCS)_2$. Studies by near-infrared–visible, infrared, and ESR spectroscopy and X-ray diffraction patterns indicate that the complexes are polymeric zigzag chains with stepwise metal–thiocyanate bridging groups and six-coordinate metal centers. Variable-temperature (1.5 to ~303 K) susceptibility measurements were made for both compounds. The presence of broad susceptibility maxima centered at ~18 K for $Mn(bpy)(NCS)_2$ and at $T < 1.5$ K for $Co(bpy)(NCS)_2$ and a rapid decrease in the moment for each compound indicate antiferromagnetic exchange in the polymer chains. Such exchange is proposed to be pairwise in nature, and with use of the Heisenberg–Dirac–Van Vleck dipolar coupling model, the exchange energy, J, is estimated to be -2.5 cm^{-1} for $Mn(bpy)(NCS)_2$.

Introduction

We have recently prepared a series of compounds with the empirical formula $M(bpy)(NCS)_2$ in which M is divalent Mn, Fe, Co, Ni, and Cu and bpy is 2,2′-bipyridine.[1] Some of the properties of two members of this series, $Cu(bpy)(NCS)_2$[1,2] and $Fe(bpy)(NCS)_2$,[1,3,4] have previously been reported. X-ray powder patterns of each system have revealed structural isomorphism between the manganese, iron, and cobalt analogues. The available data[3] indicate that $Fe(bpy)(NCS)_2$ is a polymer in which all thiocyanate groups are bridging to form zigzag chains of stepwise, nearly orthogonal

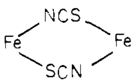

bridging groups. The structures of the present Fe, Mn, and Co compounds are most likely analogous to that recently determined for $Co(bpy)Cl_2$ in a single-crystal X-ray study[5] and are shown schematically in Figure 1a. The

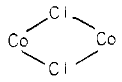

groups are found to be stepwise and nearly orthogonal. Replacement of bridging Cl^- by NCS^- should increase the metal–metal distance within the grouping from ~3.7 to ~6 Å and may change the *strength and/or sign of the magnetic exchange therein*. This will be demonstrated in the present article. However, the gross features, stepwise polymeric chains and their packing, Figure 1b, are not expected to be significantly different for $Co(bpy)Cl_2$ vs. $Co(bpy)(NCS)_2$.

From a Mössbauer spectroscopy study between 130 and 200 K,[4] $Fe(bpy)(NCS)_2$ is found to undergo a structural phase transition believed to be similar in nature to the $\alpha \rightarrow \gamma$ polymer displacement transition of the linear-chain $Co(py)_2Cl_2$ that occurs at 154 K.[6,7] For $Fe(bpy)(NCS)_2$, the transition is believed to be the result of changes in the metal–thiocyanate bridging framework from a symmetric to an asymmetric form with decreasing temperature. Below 100 K, $Fe(bpy)(NCS)_2$[3] shows evidence of low-dimensional antiferromagnetic exchange characterized by a broad maximum in χ_M' at ~18 K and relatively large negative Θ. This exchange can be explained by assuming pairwise interactions between the iron atoms in the chain. However, for the ferrous complex there is no evidence of three-dimensional antiferromagnetic ordering for T as low as 1.5 K.

The purpose of this paper is to report the electronic, magnetic, and structural properties of $Co(bpy)(NCS)_2$ and $Mn(bpy)(NCS)_2$ and to compare the properties of these two systems with the isomorphous $Fe(bpy)(NCS)_2$.

Experimental Section

The metal salts used for the preparations were reagent grade and were used without further purification. The ligand 2,2′-bipyridine

---

[1] B. W. Dockum, Ph.D. Dissertation, Northeastern University, 1977.

[2] W. M. Reiff, H. Wong, B. Dockum, T. Brennan, and C. Cheng, *Inorg. Chim. Acta*, **30**, 69 (1978).

[3] Part 1: B. W. Dockum and W. M. Reiff, *Inorg. Chem.*, **21**, 391 (1982).

[4] Part 2: B. W. Dockum and W. M. Reiff, *Inorg. Chem.*, **21**, 1406 (1982).

[5] W. M. Reiff, H. Wong, G. Eisman, W. Rode, and B. Foxman, Abstracts, 179th National Meeting of the American Chemical Society, Houston, TX, March 1980, No. INOR 22.

[6] P. J. Clarke and H. J. Milledge, *Acta Crystallogr., Sect. B*, **B31**, 1543 (1975).

[7] P. J. Clarke and H. J. Milledge, *Acta Crystallogr., Sect. B*, **B31**, 1554 (1975).

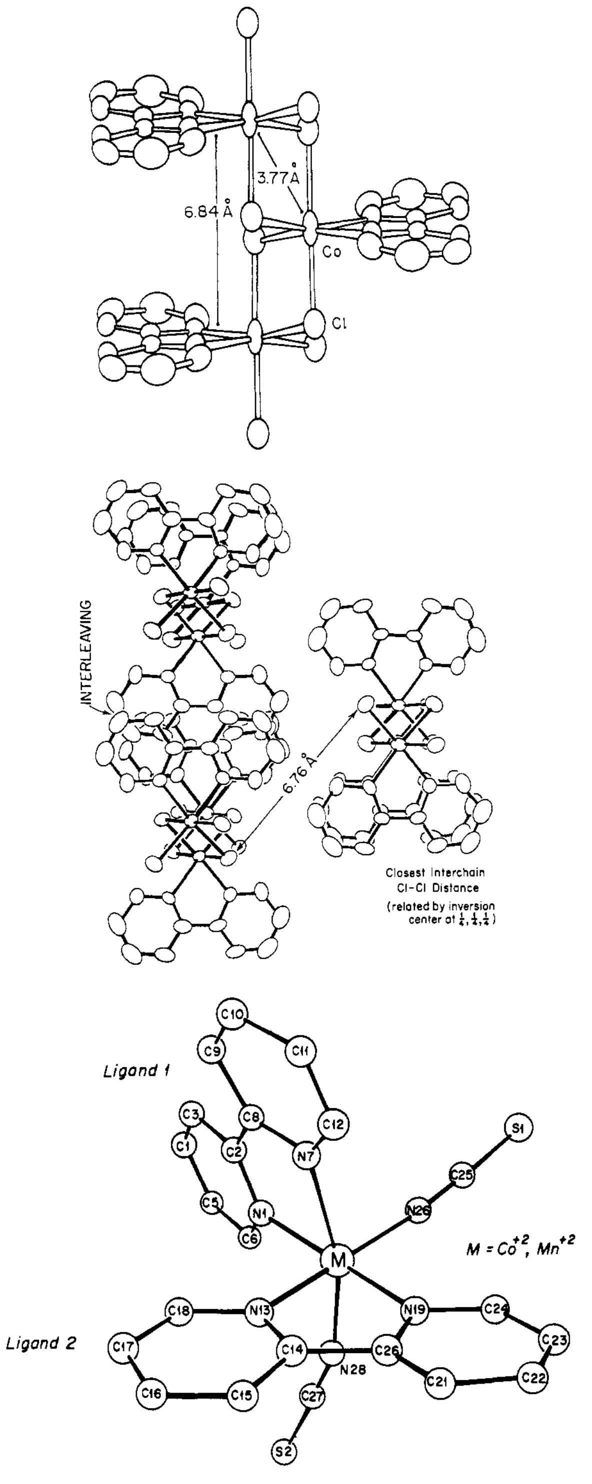

Figure 1. (a) Top: Schematic of the zigzag chain structure found by the X-ray structure determination of $Co(bpy)Cl_2$. (b) Middle: Schematic of the interleaving of adjacent chains for $Co(bpy)Cl_2$ viewed down the polymer chain axis. (c) Bottom: Schematic of the X-ray structure for the monomeric $M(bpy)_2(NCS)_2$ (M = Mn, Co).

was obtained from Columbia Organic Chemical Co., Inc. The pyridine used was reagent grade and was obtained from J. T. Baker Chemical Co. The chemical analyses were performed by Galbraith Laboratories, Knoxville, TN.

$Co(bpy)(NCS)_2$. $Co(bpy)_2(NCS)_2$ used for the preparation of $Co(bpy)(NCS)_2$ was prepared by the following method. A mixture of $CoCl_2{\cdot}6H_2O$ (1.1464 g, 4.82 mmol) and 2,2′-bipyridine (2.2669 g, 14.52 mmol) was formed in 60 mL of distilled water and was then heated to form a yellow-brown solution characteristic of the $Co(bpy)_3^{2+}$ cation. A 5-mL aqueous solution containing a twofold excess of KNCS (1.8715 g, 19.26 mmol) was added, and a brown-yellow precipitate resulted. The precipitate was washed with distilled water several times and dried under vacuum. $Co(bpy)_2(NCS)_2$ was formed by refluxing the precipitate, $Co(bpy)_3(NCS)_2$, in 500 mL of toluene for 3 days. The apricot-colored product was washed several times with fresh toluene and dried in a vacuum desiccator. The product was analyzed as $Co(bpy)_2(NCS)_2$, and the results are presented in Table I.

Table I. Elemental Analyses

compd	% calcd C	% calcd H	% calcd N	% found C	% found H	% found N
$Mn(bpy)_2(NCS)_2$	54.65	3.34	17.38	54.70	3.76	17.78
$Mn(bpy)(NCS)_2$	44.04	2.46	17.12	43.95	2.38	17.06
$Co(bpy)_2(NCS)_2$	54.21	3.31	17.24	54.43	3.54	17.26
$Co(bpy)(NCS)_2$	43.51	2.46	16.91	43.24	2.48	16.75
$Co(py)_4(NCS)_2$	53.76	4.10	17.10	52.65	4.14	16.77
$Co(py)_2(NCS)_2$	43.24	3.02	16.81	41.65	3.17	16.03

$Co(bpy)(NCS)_2$ was prepared by the high-vacuum thermolysis of $Co(bpy)_2(NCS)_2$. The bipyridine came off at ~205 °C, forming a pale gray-blue product. The thermolysis was stopped when no more bipyridine was lost as evidenced by a constancy of weight. This product was analyzed as $Co(bpy)(NCS)_2$, and the results are presented in Table I.

In some preparations, the apricot-colored product formed preferentially upon the addition of the KNCS solution to the $Co(bpy)_3^{2+}$ solution. In these instances, a large excess of thiocyanate ion was sufficient to displace 1 mol of 2,2′-bipyridine, and the ligand-extraction step with toluene was not required.

$Mn(bpy)(NCS)_2$. $Mn(bpy)_2(NCS)_2$, the precursor material for the preparation of $Mn(bpy)(NCS)_2$, was prepared by a method similar to the one for $Co(bpy)_2(NCS)_2$ except the ligand-extraction step with toluene was not required. The excess of KNCS used in the preparation was sufficient to displace 1 mol of bipyridine, and $Mn(bpy)_2(NCS)_2$ was formed directly. The results of the analysis of $Mn(bpy)_2(NCS)_2$ are given in Table I. We note here in passing that, as part of a more detailed study of the precursor *bis(bipyridine) complexes*, we have determined the structures of Mn- and $Co(bpy)_2(NCS)_2$ by single-crystal X-ray diffraction and find these compounds to be monomeric cis-isothiocyanato complexes that are isomorphous[8] (see Figure 1c).

$Mn(bpy)(NCS)_2$ was prepared by the high-vacuum thermolysis of $Mn(bpy)_2(NCS)_2$. The bis precursor was heated to ~180 °C, forming a light yellow product, $Mn(bpy)(NCS)_2$. The results of the analysis of $Mn(bpy)(NCS)_2$ are given in Table I. Since both the bis precursor and product have similar colors, the heating was stopped when the difference between the theoretical and actual ligand weight losses was within ±3 mg. The complete details of the thermolyses are given elsewhere.[1]

$Co(py)_2(NCS)_2$ (py = Pyridine). The following method was used to prepare $Co(py)_2(NCS)_2$. A quantity of anhydrous $CoCl_2$ (1.4500 g, 11.17 mmol) was dissolved in 30 mL of absolute methanol and 10 mL of 2,2′-dimethoxypropane. The resulting solution was poured into a mixture made up of 2.2008 g of (22.65 mmol) KNCS, 50 mL of absolute methanol, and 10 mL of 2,2′-dimethoxypropane. After the KCl precipitate was filtered out, the cobalt thiocyanate solution was poured rapidly into a solution of pyridine (1.8787 g, 23.66 mmol) in 15 mL of absolute methanol. A pink precipitate indicated that it was the monomeric species $Co(py)_4(NCS)_2$ (see Table I). To obtain the polymeric $Co(py)_2(NCS)_2$ for comparison of its optical spectrum to that of $Co(bpy)(NCS)_2$, it was necessary to heat the pink precipitate in an Abderhaulden apparatus for 30–45 min with toluene. The violet product was analyzed as $Co(py)_2(NCS)_2$, and the results are given in Table I.

Physical Measurements. Magnetic susceptibility measurements were determined by using the Faraday method. A description of the Faraday apparatus has been reported elsewhere.[9] The apparatus was calibrated with $HgCo(NCS)_4$.[10-12] Temperature measurement and control were based on calibrated silicon ($H = 0$) and gallium arsenide diodes ($H \neq 0$). Diamagnetic corrections to the susceptibility of $Mn(bpy)(NCS)_2$ and $Co(bpy)(NCS)_2$ were calculated from Pascal's

---

(8) M. V. Veidis, B. Dockum, F. F. Charron, Jr., W. M. Reiff, and T. F. Brennan, *Inorg. Chim. Acta*, **53**, L197 (1981).
(9) W. M. Reiff and C. Cheng, *Inorg. Chem.*, **16**, 2097 (1977).
(10) B. N. Figgis and R. S. Nyholm, *J. Chem. Soc.*, 419 (1958).
(11) H. St. Råde, *J. Phys. Chem.*, **77**, 424 (1973).
(12) D. B. Brown, V. H. Crawford, J. W. Hall, and W. E. Hatfield, *J. Phys. Chem.*, **81**, 1303 (1977).

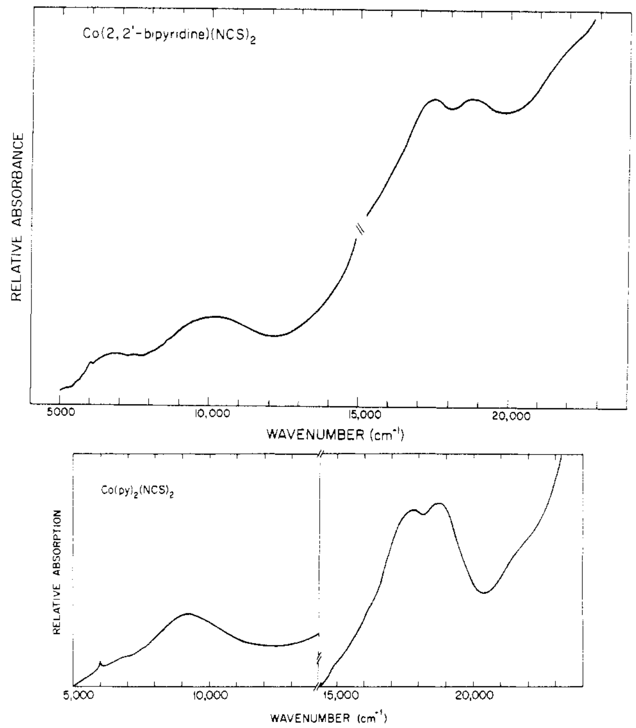

Figure 2. Near-infrared–visible spectra of (a, top) Co(bpy)(NCS)$_2$ and (b, bottom) Co(py)$_2$(NCS)$_2$.

Table II. Near-Infrared-Visible Band Maxima

compd	band max, cm^{-1} (rel intens)[a]	ref
Co(bpy)(NCS)$_2$	6750 (w), 10 200 (w), ~14 800 (sh), 17 500 (s), 18 750, 21 750 (sh)	b
Co(py)$_2$(NCS)$_2$	~6500 (w), 9260 (s), ~15 100 (sh), 16 030 (sh), 17 800 (vs), 18 730 (vs), 21 740 (sh)	b
Co(2,9-dmp)Cl$_2$	6450 (s, sh), 7650 (s), 10 400 (m), 15 150 (vs), 17 450 (s), 18 300 (sh), 23 650 (sh)	1, 15

[a] w = weak, s = strong, sh = shoulder, m = medium, and vs = very strong. [b] This work.

Table III. Infrared Spectral Results (cm^{-1})[a] for Co(bpy)(NCS)$_2$, Co(bpy)$_2$(NCS)$_2$, Mn(bpy)(NCS)$_2$, and Mn(bpy)$_2$(NCS)$_2$

Co(bpy)-(NCS)$_2$	Co(bpy)$_2$-(NCS)$_2$	Mn(bpy)-(NCS)$_2$	Mn(bpy)$_2$-(NCS)$_2$	assignt
2112 (sh)		2136 (w, sh)		
2093	2093 (sh)	2108		
2064	2085	2086	2059	N-C str, ν_1(NCS)
	2075	2062	2050	
	2020 (sh)	2008 (w, sh)		
812 (w)	810 (sh)	814 (vw)		C-S str, ν_3(NCS)
798 (m)	796 (m)	788 (w)		
474 (s)	472	473		N-C-S bend, δ(NCS)
434 (w)				
414 (s)		416		bpy bend
	306			
291				
282		269 (sh)		
269		257		Co-N(NCS) str
250		250		Co-N(bpy) str
222		223 (sh)		
202				

[a] w = weak, s = strong, sh = shoulder, m = medium, and vs = very strong.

constants.[13] For each compound $\chi_{diam} = -180 \times 10^{-6}$ cgsu mol^{-1}.

Near-infrared–visible spectra were taken on a Cary 14 recording spectrometer. Samples were prepared as mulls of finely ground compound in Halocarbon 25-5S grease (Halocarbon Products Corp., Hackensack, NJ); the sample mull was suspended between two UV grade quartz plates.

Infrared spectra between 4000 and 200 cm^{-1} were obtained on a Perkin-Elmer Model 567 spectrometer. Samples were taken as mineral-oil mulls on either a single NaCl plate or a single polyethylene disk and as KBr pellets.

Comparative ESR spectra were determined at ambient temperature with a Bruker Instruments Co. ER-10 X-band spectrometer calibrated relative to the center of the hyperfine pattern of divalent manganese in Plasticene. Differential-scanning calorimetry measurements were made with a Perkin-Elmer Model DSC-1B.

To conclude this section, we point out that to date we have been unable to obtain single crystals for any of the M(bpy)(NCS)$_2$ systems suitable for structure determination. The products resulting from the thermolytic preparation are finely divided powders that give broad diffractometer peaks. In addition, we find that these products either are generally insoluble or appear to disproportionate in our attempts to recrystallize them from various solvents. Finally, we have not been successful in the direct-solution preparation of any M(bpy)(NCS)$_2$ compound except for the case of copper.[2]

Results and Discussion

Optical Spectra. The optical spectra for Co(bpy)(NCS)$_2$ and Co(py)$_2$(NCS)$_2$ are presented in Figure 2. The band maxima for each compound are given in Table II. Comparison of the spectrum of each compound shows they are quite similar, i.e., bands at ~6500 and ~9000–10 000 cm^{-1}, shoulders at ~15 000 and ~21 500 cm^{-1}, and two intense bands at ~18 000 cm^{-1} (see Table II). It is known from a single-crystal X-ray study[14] that Co(py)$_2$(NCS)$_2$ is a linear-chain polymer articulated from

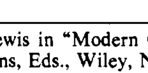

units via bridging thiocyanate groups with trans axial pyridine ligands resulting in a pseudooctahedral CoN$_2$N'$_2$S$_2$ chromophore having approximately D_{2h} local symmetry. The gross similarity of the two spectra indicates that Co(bpy)(NCS)$_2$ also contains a pseudooctahedral CoN$_2$N'$_2$S$_2$ chromophore of comparable ligand field strength as Co(py)$_2$(NCS)$_2$. However, an exact correspondence of the two spectra is not expected because of inherently lower symmetry of the CoN$_2$N'$_2$S$_2$ chromophore in Co(bpy)(NCS)$_2$ resulting from the *cis coordination* of the imine nitrogen atoms of 2,2'-bipyridine. As will be seen subsequently, Co(bpy)(NCS)$_2$ is found to have bridging thiocyanates from infrared evidence further supporting the proposal of a pseudooctahedral CoN$_2$N$_2$'S$_2$ chromophore. Before this section is concluded, the possibility of a pseudotetrahedral cobalt center should also be considered briefly for Co(bpy)(NCS)$_2$. The optical spectrum of (2,9-dimethyl-1,10-phenanthroline)cobalt(II) chloride, a known pseudotetrahedral cobalt(II) compound with a CoN$_2$Cl$_2$ chromophore,[15] shows two very intense bands at 7650 and 15 150 cm^{-1} (see Table II), which on comparison are not observed in the spectrum of Co(bpy)(NCS)$_2$. These intense bands are characteristic of *Laporte-allowed* d–d transitions in tetrahedral cobalt(II). The steric hindrance for the dimethyl ligand prevents the attainment of six-coordination via polymerization as suggested for Co(bpy)(NCS)$_2$.

Infrared Spectra. The infrared spectrum of each mono complex, M(bpy)(NCS)$_2$, was determined. The most important bands along with their probable assignments are

---

(13) B. N. Figgis and J. Lewis in "Modern Coordination Chemistry", J. Lewis and R. G. Wilkins, Eds., Wiley, New York, 1960, p 403.

(14) M. A. Porai-Koshits and G. N. Tishchenko, *Sov. Phys.—Crystallogr.* (*Engl. Transl.*), **4**, 216 (1980).

(15) D. B. Fox, J. R. Hall, and R. A. Plowman, *Aust. J. Chem.*, **18**, 691 (1965).

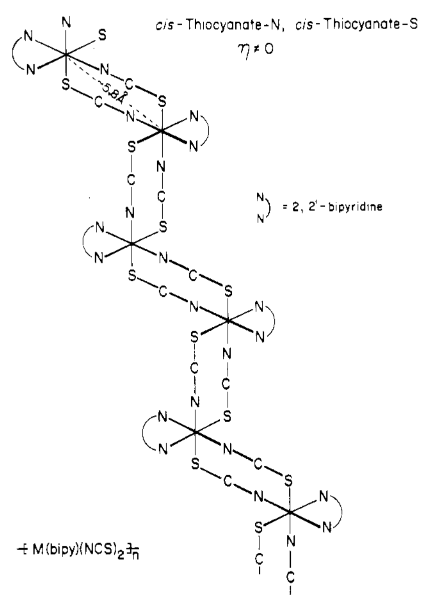

Figure 3. Proposed polymer structure for $Mn(bpy)(NCS)_2$ and $Co(bpy)(NCS)_2$.

presented in Table III. In thiocyanate compounds, the intense bands found at ~2000 cm^{-1} are assigned to the C–N stretching mode of the thiocyanate anion. The exact position of this band can give some information about the metal–thiocyanate coordination. Two intense bands are found in this region for each of the mono(bipyridyl) compounds: $Mn(bpy)(NCS)_2$, 2086 and 2108 cm^{-1}; $Co(bpy)(NCS)_2$, 2093 and 2112 cm^{-1}. This band pattern is consistent with, but is not unequivocably proof of, the presence of bridging thiocyanate anions[15,16] in the present compounds.

ESR Spectra. The ESR spectra of $Mn(bpy)(NCS)_2$ and $Mn(bpy)_2(NCS)_2$ were measured at room temperature. Each spectrum showed a single signal centered at $g = 2$. However, the spectrum for $Mn(bpy)(NCS)_2$ exhibited a broader signal that was an order of magnitude *less intense* than that of the monomer. Such behavior is often observed in dimeric or polymeric compounds that undergo exchange interactions between metal atoms resulting in broad ESR signals of low intensity. This g value is at first glance surprising since $g = 2$ implies an isotropic manganese electronic environment with negligible zero-field splitting of the ground spin sextet. A regular structure for $Mn(bpy)(NCS)_2$, one of high symmetry, is not likely from a consideration of the infrared and X-ray diffraction data, which imply a polymer structure for $Mn(bpy)(NCS)_2$. ESR studies by Dowsing et al.[17] have demonstrated that polymers such as bis(γ-picoline)manganese(II) chloride and bis(quinoline)manganese(II) chloride exhibit a single ESR resonance at $g \sim 2$. While the local symmetry is low in these systems and additional ESR transitions are expected from axial and/or rhombic single-ion zero-field splitting, magnetic interactions between neighboring manganese atoms obscure their observation. Hence, the ESR data are fully consistent with the proposed polymer structure for $Mn(bpy)(NCS)_2$ with significantly broadening magnetic exchange interactions.

Structure of $Mn(bpy)(NCS)_2$ and $Co(bpy)(NCS)_2$. The spectroscopic data presented earlier plus the X-ray powder data lead to the conclusion that $Mn(bpy)(NCS)_2$ and $Co(bpy)(NCS)_2$ are isomorphous polymers with bridging thiocyanate ligands and six-coordinate centers. A probable structure for $Mn(bpy)(NCS)_2$ and $Co(bpy)(NCS)_2$ is the zigzag chain previously proposed for $Fe(bpy)(NCS)_2$[1,3] (see Figure 3) and found in an X-ray study of $Co(bpy)Cl_2$.[5] The chain is generated from

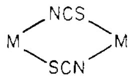

units as found in the linear-chain polymers $Co(py)_2(NCS)_2$,[14] $Cu(py)_2(NCS)_2$,[14] $Co(NCS)_2{\cdot}3H_2O$,[18] and $Ni(2\text{-thioimidazolidine})_2(NCS)_2$.[19] However, there is a stepwise arrangement in which these bridging units are nearly orthogonal to each other. This arrangement is a consequence of the cis coordination of 2,2′-bipyridine nitrogen atoms to the metal. The metal–metal distance between nearest metal neighbors is estimated to be ~6.0 Å from comparisons with the foregoing linear-chain polymers and nickel dimers containing thiocyanate bridging.[20,21] Another structure possibility that is not ruled out by the present investigation is an infinite, helical polymer with thiocyanate bridging as found in an X-ray study of bis(thioacetamide)nickel(II) thiocyanate.[22]

The existence of a structural phase transition in either $Mn(bpy)(NCS)_2$ or $Co(bpy)(NCS)_2$ cannot be concluded at this time. Additional ESR spectra of $Mn(bpy)(NCS)_2$ taken at 78 K showed a single, broad transition at $g \sim 2$, which was similar to the spectrum at room temperature and generally uninformative. Differential-scanning calorimetry studies of $Mn(bpy)(NCS)_2$, $Co(bpy)(NCS)_2$, and $Fe(bpy)(NCS)_2$ over the range 125–300 K were made and did not reveal endotherms (increasing T) or exotherms (decreasing T) that can be associated with a structural phase transition. Such endotherms are observed in our DSC study[23] of the $\gamma \rightarrow \alpha$ transitions of Mn-, Fe-, and $Co(py)_2Cl_2$ for *crystalline solution preparations* of the compounds. Previous discussions[4] of the phase transition in $Fe(bpy)(NCS)_2$ imply that it is first order, but it occurs over a large temperature range because of defects in the crystal structure (broken metal-bridging bonds). Such defects are readily generated by the high-temperature, thermolytic preparation of each system. These defects can broaden the temperature range over which the phase transition occurs and prevent its observation via usual thermal methods. Additional differential-scanning calorimetry investigations using more crystalline samples (e.g., the product of solution-preparative methods if such are devised) of each compound may reveal the phase transition in the manganese and cobalt analogues. The temperature dependence of Mössbauer spectra using ^{57}Fe-doped samples or a $Co(bpy)(NCS)_2$ emission source may also reveal a structural phase transition. Such studies have revealed the *polymer displacement* transformations in $Mn(py)_2Cl_2$,[24] $Ni(py)_2Cl_2$,[24] and $Co(py)_2Cl_2$[25] and are topics for future work in this laboratory for the present complexes.

Magnetic Properties. Magnetic susceptibility data for both compounds have been determined for 10 fields ranging between 1.66 and 5.10 kG with a Faraday balance. Plots of χ_M', $\chi_M'^{-1}$, and μ vs. T for 5.1 kG are given in Figures 4 and 5 for $Mn(bpy)(NCS)_2$ and $Co(bpy)(NCS)_2$, respectively. We have also determined the susceptibility of $Mn(bpy)(NCS)_2$ for larger fields up to ~14 kG with a vibrating sample magnetometer,

---

(16) R. J. H. Clark and C. S. Williams, *Spectrochim. Acta*, **22**, 1081 (1966).

(17) R. D. Dowsing, J. F. Gibson, D. M. L. Goodgame, M. Goodgame, and P. J. Haywood, *Nature (London)*, **219**, 1037 (1968).

(18) F. H. Cano, S. Garcia-Blanco, and A. Guerrerc-Laverat, *Acta Crystallogr., Sect. B*, **B32**, 1526 (1976).

(19) M. Nardelli, G. F. Gasparri, A. Musatti, and A. Manfredotti, *Acta Crystallogr.*, **21**, 910 (1966).

(20) A. P. Ginsberg, R. L. Martin, R. W. Brooks, and R. C. Sherwood, *Inorg. Chem.*, **11**, 2884 (1972).

(21) A. E. Shvzlashvili, M. A. Porai-Koshits, and A. S. Antsyshkina, *J. Struct. Chem. (Engl. Transl.)*, **10**, 552 (1969).

(22) L. Capacchi, G. F. Gasparri, M. Nardelli, and G. Pelizzi, *Acta Crystallogr., Sect. B*, **B24**, 1199 (1968).

(23) G. A. Eisman and W. M. Reiff, *Inorg. Chim. Acta*, **44**, L171 (1980).

(24) T. Yoshihashi and H. Sano, *Chem. Phys. Lett.*, **34**, 289 (1975).

(25) J. P. Sanchez, L. Asch, and J. M. Friedt, *Chem. Phys. Lett.*, **18**, 250 (1973).

Table IV. Results of Least-Squares Computer Fits of $\chi_M'^{-1} = (T - \Theta)/C$

compd	μ_{eff}, μ_B	C, emu/mol	Θ, K	temp range, K
$Fe(bpy)(NCS)_2$	5.59 (5.72)	3.90 (4.10)	−29.2 (−27.8)	77–300 (50–100)
$Mn(bpy)(NCS)_2$	5.98 (6.20)	4.47 (4.81)	−41.2 (−41.9)	77–300 (50–100)
$Co(bpy)(NCS)_2$	4.73 (4.81)	2.79 (2.90)	−8.5 (−9.8)	77–300 (50–100)

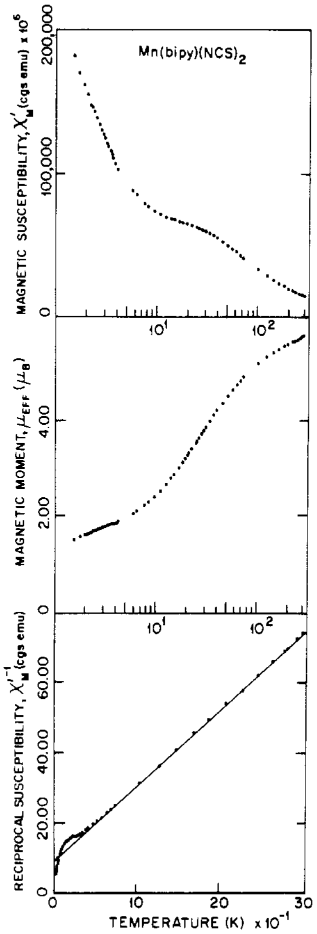

Figure 4. Plots of the magnetic data vs. temperature: (a, top) χ_M' vs. T, (b, middle) μ vs. T, and (c, bottom) $\chi_M'^{-1}$ vs. T for $Mn(bpy)(NCS)_2$ measured between 0 and 100 by using a field of 5.1 kG (data obtained with a Faraday balance).

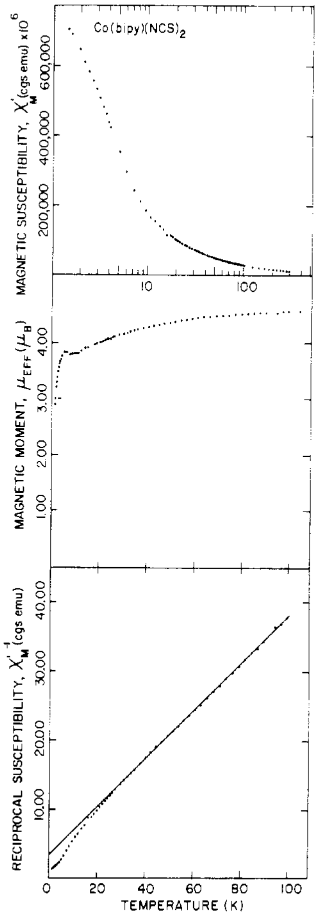

Figure 5. Plots of the magnetic data vs. temperature: (a, top) χ_M' log T, (b, middle) μ vs. T, and (c, bottom) $\chi_M'^{-1}$ vs. T for $Co(bpy)(NCS)_2$ measured between 0 and 100 K by using a field of 5.1 kG (data obtained with a Faraday balance).

Table V. Sample Moment Data for $Mn(bpy)(NCS)_2$

T, K	μ, μ_B	T, K	μ, μ_B	T, K	μ, μ_B
302.22	5.73	20.80	3.26	3.57	1.81
283.07	5.71	18.55	3.10	3.43	1.80
264.88	5.68	15.19	2.85	3.31	1.78
227.91	5.63	12.77	2.65	3.16	1.77
188.16	5.53	9.64	2.38	3.03	1.75
147.69	5.39	8.43	2.27	2.91	1.74
104.12	5.16	8.38	2.26	2.77	1.72
69.13	4.81	7.81	2.21	2.61	1.70
57.81	4.62	6.46	2.10	2.48	1.68
46.21	4.35	5.89	2.03	2.40	1.67
37.71	4.09	4.20	1.85	2.28	1.64
31.58	3.84	4.20	1.87	2.12	1.62
28.48	3.70	4.00	1.84	1.96	1.59
25.68	3.55	3.80	1.82	1.75	1.54
22.74	3.38	3.70	1.82	1.55	1.50

and these data are shown in Figure 6. Least-squares computer fits of $\chi_M'^{-1}$ vs. T show the compounds to obey generally similar Curie–Weiss laws between 78 and 300 K and between 50 and 100 K. These latter fits correspond to independent susceptibility determinations for different samples over the temperature ranges 78–300 and 4.2–100 K, respectively. The susceptibility data are examined in this manner because, at least in the case of $Fe(bpy)(NCS)_2$, there are clearly two structural forms of the compound present and coexisting over the range ~130–200 K owing to the structural phase transformation mentioned earlier. The data suggest that the Curie–Weiss law parameters are not significantly different for the two forms of the latter compound. As yet, we have no direct evidence of a similar structural phase transformation for the isomorphous cobalt and manganese analogues, and further speculation on this point now is unwarranted. For $Co(bpy)(NCS)_2$, a nonlinear least-squares fitting procedure leads to a *temperature-independent paramagnetic contribution* to χ_M' of 225×10^{-6} cgsu. After correction for the latter, least-squares fits to $\chi_M'^{-1}$ vs. T yield $\mu_{eff} = 4.64$ μ_B, $C = 2.70$ emu/mol, and $\Theta = -4.97$ K, suggesting relatively weak antiferromagnetic interaction. The results of these fits for each compound, as well as those for $Fe(bpy)(NCS)_2$, are given in Table IV. Lists of the moment data are given in Tables V and VI for $Mn(bpy)(NCS)_2$ and $Co(bpy)(NCS)_2$. It is clear that simple Curie laws do not apply.

The susceptibility of $Mn(bpy)(NCS)_2$ approaches a broad maximum at ~20 K and then begins to rise sharply at lower temperatures. The broad maximum in χ_M' and large negative Θ (see Table IV) signify substantial antiferromagnetic interaction at lower temperatures. The rise in the susceptibility at even lower temperatures may represent the contribution of

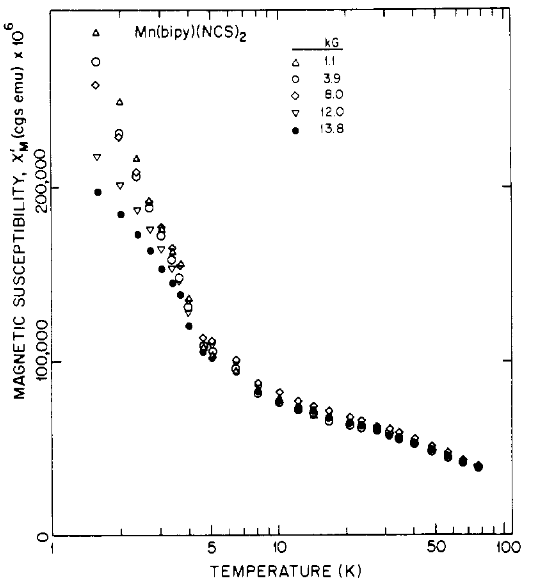

Figure 6. Plots of χ_M' vs. log T in the range ~1.5 to 100 K for fields varying from 1.1 to 13.8 kG (data obtained with a vibrating-sample magnetometer).

Table VI. Sample Moment Data for Co(bpy)(NCS)$_2$

T, K	μ, μ_B	T, K	μ, μ_B	T, K	μ, μ_B
302.73	4.69	44.66	4.35	8.55	3.80
265.26	4.73	40.37	4.30	7.44	3.80
228.26	4.63	35.69	4.24	6.18	3.85
188.45	4.58	32.82	4.21	5.22	3.84
147.68	4.64	29.75	4.16	4.20	3.87
104.17	4.57	26.20	4.11	4.00	3.85
97.06	4.57	23.40	4.07	3.76	3.83
89.77	4.55	21.18	4.03	3.51	3.80
84.62	4.53	18.74	3.98	3.25	3.75
79.35	4.52	17.75	3.98	2.99	3.69
73.98	4.50	16.33	3.94	2.75	3.62
68.70	4.48	14.94	3.91	2.47	3.50
63.24	4.47	13.92	3.91	2.23	3.41
58.64	4.43	12.24	3.85	2.00	3.31
53.99	4.40	11.07	3.81	1.64	3.08
49.27	4.36	9.83	3.82	1.50	2.96

paramagnetic impurities to the susceptibility, e.g., a trace of the Mn(bpy)$_2$(NCS)$_2$ precursor. However, this point will be discussed further subsequently. The effects of the antiferromagnetic interaction can also be observed in the moment–temperature variation (see Table V). At 302.80 K, the moment is 5.83 μ_B, slightly below the expected spin-only value of 5.92 μ_B; at 4.2 K, μ = 1.60 μ_B. The latter value is considerably lower than that expected (~$19^{1/2}$) if only single-ion, zero-field-splitting effects are operative[26] and again suggests antiferromagnetic exchange.

The log scale plot of the low-temperature susceptibility of Co(bpy)(NCS)$_2$ appears to approach a maximum below 1.5 K; however, we then reach the limit of our low-T capabilities. This result, along with the small negative Θ (see Table IV), probably indicates a weak overall antiferromagnetic interaction. However, any antiferromagnetic exchange for Co(bpy)(NCS)$_2$, if present, appears to be substantially weaker than for Mn(bpy)(NCS)$_2$ or Fe(bpy)(NCS)$_2$, i.e., as gauged by a lower negative Θ value. It is clear that the magnetic behavior is complex and may well be dominated by (1) single-ion spin–orbit and zero-field-splitting effects as opposed to (2) antiferromagnetic exchange or (3) a combination of effects 1 and 2 with $D \sim J$. The effective moment from the Curie–Weiss fit, μ_{eff} = 4.81 μ_B, is greater than the spin-only value of 3.89 μ_B ($15^{1/2}$, $S = {}^3/_2$), indicating residual orbital momentum contribution to the moment. This moment value lies in the lower end of the range expected for octahedral cobalt(II),[27] consistent with the distorted six-coordinated cobalt center mentioned earlier (see Table VI).

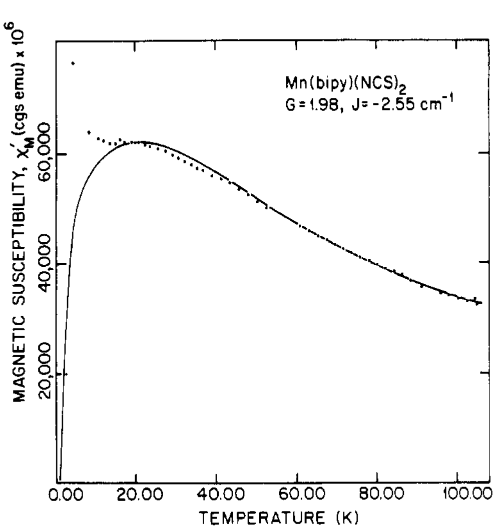

Figure 7. Plot of χ_M' vs. T for Mn(bpy)(NCS)$_2$, which includes the calculated χ_M' obtained by the Heisenberg–Dirac–Van Vleck dipolar coupling model using the value of g = 1.98 and J = −2.5 cm^{-1}.

As noted before, the broad maximum in the susceptibility of Mn(bpy)(NCS)$_2$ indicates the presence of antiferromagnetic interactions in the compound. Depending on the lattice dimensionality, the susceptibility maximum may result from substantial negative exchange within 2-D layers, 1-D linear chains, or small clusters of interacting spins. The exchange within the chains and layers may be determined by the use of the Heisenberg, Ising, or XY model.[28,29] Since the Mn^{2+} ion has a nondegenerate (^{6}A) orbital ground state in a weak crystal field with a g value very close to 2, an isotropic Heisenberg model for a linear chain may be used to estimate the intrachain exchange in Mn(bpy)(NCS)$_2$. Unfortunately, with the Heisenberg model, no exact solution is available for a linear array of atoms of $S = {}^5/_2$, much less for a zigzag array as in the present case. However, by the use of a scaling procedure, expressions 1 and 2 for the susceptibility for S =

$$\chi = \frac{Ng^2\mu^2}{3kT}S(S+1)\left(\frac{1+u}{1-u}\right) \qquad u = \coth A - \frac{1}{A} \qquad A = \frac{2JS(S+1)}{kT} \tag{1}$$

$$\frac{|J|\chi_{max}}{Ng^2\mu^2} = 0.1004 \qquad \frac{kT_{max}}{|J|} = 8.2 \tag{2}$$

${}^5/_2$ may be obtained by using the Heisenberg model.[30] The quantities N, μ_B, k, T, S, and J have their usual meanings. In eq 2, χ_{max} refers to the maximum value of the susceptibility found in the broad susceptibility maximum, and T_{max} corresponds to the temperature at which χ_{max} is found. With use of eq 2, an estimate of the intrachain exchange energy, J, and g value may be determined. For Mn(bpy)(NCS)$_2$ (χ_{max} = 62000 × 10^{-6} cgsu mol^{-1} and T_{max} = ~16 K), J and g are the following: $|J/k|$ = −1.93 (J = −1.35 cm^{-1}); g = 1.79. The g value determined by this calculation is much lower than 2, and a model based on a linear chain is probably not applicable to a system containing zigzag polymer chains as proposed for

---

(26) C. Maricondi, W. Swift, and D. K. Straub, *J. Am. Chem. Soc.*, **91**, 5205 (1969).

(27) R. L. Carlin, *Transition Met. Chem.*, **1**, 1 (1965).

(28) L. J. DeJongh and A. R. Miedema, *Adv. Phys.*, **23**, 87 (1976).

(29) M. Steiner, J. Villian, and G. G. Windsor, *Adv. Phys.*, **25**, 87 (1976).

(30) G. R. Wagner and S. A. Friedberg, *Phys. Lett.*, **9**, 11 (1964).

$Mn(bpy)(NCS)_2$. The nearly orthogonal, stepwise bridging groups proposed for the zigzag chain are expected to prevent extensive, longer range, metal–metal interactions as found in the linear-chain systems. The magnetic properties in $Mn(bpy)(NCS)_2$ are then more appropriately interpreted in terms of the interaction of pairs of metal atoms that constitute the zigzag chain. If the interactions between such clusters are weak or zero, the antiferromagnetic exchange energy, J, can be determined to the first order by using the Heisenberg–Dirac–Van Vleck dipolar coupling model that is usually applied to simple dimers. For $Mn(bpy)(NCS)_2$, the equation for the susceptibility (per metal atom) using this model for a spin $S = {}^5/_2$ is shown by (3),[31] where $x = -J/kT$ (J is the exchange

$$\chi_M = \frac{Ng^2\mu_B{}^2}{3kT} \times \left(\frac{165 + 90e^{10x} + 42e^{18x} + 15e^{24x} + 3e^{28x}}{11 + 9e^{10x} + 7e^{18x} + 5e^{24x} + 3e^{28x} + e^{30x}} \right) + N\alpha \quad (3)$$

energy, $|2J|$ represents the singlet–triplet splitting, and $N\alpha$ represents the temperature-independent paramagnetism). All other terms have their usual meaning. Figure 7 shows the plot of both the observed magnetic data measured in a magnetic field of 5.10 kG and the susceptibilities calculated from eq 3 with $g = 1.98$ and $J = -2.6$ cm^{-1} determined from a fit done between 10.5 and 303 K with $N\alpha = 0$. The g value obtained from this least-squares fit is very close to 2, which is expected for manganese(II) and consistent with our ESR results. The dipolar model seems to represent adequately the magnetic data above 10 K. Our application is not the first example of the use of the dipolar model to interpret the magnetic data of polymer systems. Another example is the salt $Cu(NO_3)_2 \cdot 2.5H_2O$, which has a structure containing a zigzag array of copper atoms bridged by oxygen atoms from water.[32] Studies by magnetic susceptibility,[33] heat capacity,[34] and proton magnetic resonance measurements[35] have shown that a simple dipolar model of dimer-like clusters can approximately represent the magnetic data of $Cu(NO_3)_2 \cdot 2.5H_2O$. A more complete analysis of the data has shown that interpair interactions are necessary to give better agreement between theory and experiment while ESR data have favored a magnetic ladder-model structure for $Cu(NO_3)_2 \cdot 2.5H_2O$.[36] A simple dimer model has also been used to interpret the magnetic data in the copper polymer $Cu(NH_3)_2CO_3$,[38] the linear-chain system $Fe(C_2O_4) \cdot 2H_2O$,[39] and the iron analogue of $Mn(bpy)(NCS)_2$, $Fe(bpy)(NCS)_2$.[1,3] It is expected that the pairwise dipolar model could also account for the magnetic data of $Co(bpy)(NCS)_2$, but with an antiferromagnetic exchange energy smaller than that for manganese and iron analogues. No attempt was made to fit the susceptibility data for $Co(bpy)(NCS)_2$ because of the necessity to incorporate the complicating effects of a large spin–orbit coupling, a zero-field splitting, and a low-symmetry component into the Heisenberg–Dirac–Van Vleck dipolar coupling model, where the foregoing effects may be comparable to the magnetic exchange.

As mentioned earlier, the rise in χ_M' vs. T at our lowest temperatures for $Mn(bpy)(NCS)_2$ may be due in part to the presence of trace paramagnetic impurities. On the other hand, the rise is very rapid and the possibility of the onset of weak, extended, three-dimensional magnetic ordering should be considered. In view of the proposed structure, such cooperative ordering is expected at very low temperatures. The field dependence of χ_M' evident in the vibrating-sample magnetometer data below ~4 K (Figure 6) suggests the foregoing possibility. Over comparable field ranges (0 ~ 5 kG), the Faraday balance and vibrating-sample magnetometer data are essentially the same. However, at the higher fields available with our vibrating-sample apparatus, there is a clearly exhibited field dependence that is surprisingly reminiscent of a three-dimensionally ordered ferromagnetic material. That is, at fixed T, one has an inverse susceptibility vs. field behavior that is dictated by the demagnetizing behavior of the sample. The field dependence of the molar susceptibility is the result of a demagnetizing field acting within a sample to counter the applied magnetic field. The magnitude of the demagnetization depends on the shape of the sample as well as the strength of the magnetization within the material. The effect of the demagnetization field on the susceptibility is to create the observed inverse field dependence as depicted in Figure 6. A further consequence of the demagnetizing field is that the susceptibility levels off at some finite temperature. We speculate that a possible origin for the preceding field dependence is the incomplete cancellation of the spin moments in the antiferromagnetically coupled

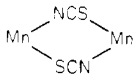

dimer pairs constituting the polymer chain. A weak positive exchange interaction between nonzero resultant moments of successive pairs could then potentially lead to the observed behavior.

Conclusion. To conclude this work, we point out that difficulty in synthesizing mono(bipyridyl) complexes of first-transition-series metals by using solution methods is not unexpected. One is confronted with the thermodynamics of the chelate effect favoring the formation of tris or bis species. Those diimine ligands (e.g., 2,9-dimethylphenanthroline, 2,2′-biquinoline) that allow ready formation of monochelate complexes are too sterically hindered to lead to magnetically interesting polymers. In addition to yielding finely divided polycrystalline products, the present thermolysis preparations suffer from the possibility of the introduction of defects. These defects can significantly affect low-temperature magnetic properties, in particular cooperative ordering, while having little or no noticeable effect on ordinary spectral properties and X-ray powder patterns. In an effort to avoid these complications and in the hope of obtaining single-crystal samples of the $M(bpy)(NCS)_2$ systems, we are currently pursuing preparation and crystal growth by gel diffusion–slow mixing of reactants.

Acknowledgment. The authors wish to acknowledge the support of the National Science Foundation, Division of Materials Research, Solid State Chemistry Program, Grant No. DMR-80-12625. They also express their appreciation to Dr. Arthur Heis of Bruker Instruments, Inc., Billerica, MA, for his assistance in obtaining X-band ESR spectra.

Registry No. $Mn(bpy)_2(NCS)_2$, 83586-95-1; $Mn(bpy)(NCS)_2$, 83586-97-4; $Co(bpy)_2(NCS)_2$, 83648-22-0; $Co(bpy)(NCS)_2$, 83586-99-6; $Co(py)_4(NCS)_2$, 14882-22-5; $Co(py)_2(NCS)_2$, 30662-39-6; $Fe(bpy)(NCS)_2$, 79803-24-0.

---

(31) W. Wojciechowski, *Inorg. Chim. Acta*, **1**, 319 (1967). Note: The susceptibility equations in this reference are for 1 mol of *dimer* and are derived on the basis of the Hamiltonian $-JS_1 \cdot S_2$, giving a singlet–triplet splitting of $|J|$. Equation 1 of this work, calculated by using the Hamiltonian $-2JS_1 \cdot S_2$, is based on 1 mol of *metal* and may be obtained from the equation in the above reference by multiplying it by ${}^3/_2$ and replacing each x by $2x$.

(32) B. Morosin, *Acta Crystallogr., Sect. B*, **B26**, 1203 (1970).

(33) L. Berger, S. A. Friedberg, and J. T. Schriempf, *Phys. Rev.*, **132**, 1057 (1963).

(34) S. A. Friedberg and C. A. Raquet, *J. Appl. Phys.*, **39**, 1132 (1968).

(35) S. Wittekoek and N. J. Poulis, *J. Appl. Phys.*, **39**, 1017 (1968).

(36) J. C. Bonner and S. A. Friedberg, *AIP Conf. Proc.*, **18** (2), 1311 (1973).

(37) J. Eckert, D. E. Cox, G. Shirane, S. A. Friedberg, and H. Kobayashi, *Phys. Rev. B: Condens. Matter*, **20**, 4596 (1979), and references within.

(38) D. Y. Jeter, D. J. Hodgson, and W. E. Hatfield, *Inorg. Chem.*, **11**, 185 (1972).

(39) J. T. Wrobleski and D. B. Brown, *Inorg. Chem.*, **18**, 2738 (1979).